Eur. Phys. J. D (2015) 69: 177
DOI: 10.1140/epjd/e2015-60186-4

THE EUROPEAN PHYSICAL JOURNAL D

Regular Article

Structural and mechanic properties of $RFeO_3$ with R = Y, Eu and La perovskites: a first-principles calculation

M. Romero[1,a], R. Escamilla[2,3], V. Marquina[1], and R. Gómez[1]

[1] Facultad de Ciencias, Universidad Nacional Autónoma de México, Apartado Postal 70-399, 04510 México D.F., México
[2] Instituto de Investigaciones en Materiales, Universidad Nacional Autónoma de México, Apartado Postal 70-360, 04510 México D.F., México
[3] ESIME-Culhuacán, Instituto Politécnico Nacional, Av. Santa Ana 1000, C.P. 04430, México, D.F., México

Received 18 March 2015 / Received in final form 15 May 2015
Published online 19 July 2015 – © EDP Sciences, Società Italiana di Fisica, Springer-Verlag 2015

Abstract. The structural and elastic properties of the RFeO$_3$ phases with R = Y, Eu, and La were investigated using first-principles plane-wave pseudopotential density functional theory with the generalized gradient approximation (GGA). The ground state properties (equilibrium cell constants) agree well with the reported experimental results. Our results showed an increase in the unit-cell volume (V) with the increase of ionic radii. We calculate a set of elastic parameters (bulk modulus B_{VRH}, shear modulus G_{VRH}, Young's modulus E_{VRH} and Poisson's ratio ν) in the framework of the Voigt-Reuss-Hill (VRH) approximation. The sound velocities (v_l, v_t) and Debye temperature (θ_D) were calculated using these elastic moduli. The calculated elastic constants were positives and satisfy the well-known Born criteria, indicating that the orthorhombic structure is stable. Finally, the ratio G_{VRH}/B_{VRH} suggests that the RFeO$_3$ phases are ductile in nature.

1 Introduction

The discovery, in the early nineteenth century, of a mineral with a chemical formula $CaTiO_3$ [1], called perovskite, gave rise to the family of compounds called orthoferrites, with general chemical formula $RFeO_3$ where R is a rare earth. This perovskites have attracted much attention due to their technological applications; for example, they are suitable candidates for electronic applications due to they mixed conductivity, they can be used as chemical sensors for the detection of gas [2], they are useful for fuel cells in the solid state [3], they can act as electrode materials in solid oxide fuel cells [4,5], as memory devices and they have spintronic applications [6–8]. An important property of some ABO_3 materials, relevant to this work, is that an epitaxial strain can have profound effects on the ferroelectric and ferromagnetic properties of thin films [9,10].

These materials are considered as strongly correlated electron systems, in which the narrow bands of $3d$ transition metals (TM) and rare earth $4f$ (R) orbitals interact through strong Coulomb repulsion U. This interaction generates unusual electronic, magnetic, optical, and sometimes even mechanical properties. The structural and electronic properties of the $RFeO_3$ compounds, with R = Y, Eu, and La, have been studied experimentally [11–13] and theoretically [14–16]; however, the study of their elastic properties has not been carrying out. In consequence, the study of their structural and elastic properties is required to know and understand their physical properties and perhaps predict new ones. The outline of the paper is the following: In Section 2 we present the technical details of the employed methods in our calculations. Section 3 describes the structural properties of the different members of this system. In Section 4, we calculate the elastic constants C_{ij}, the bulk (B_{VRH}), shear (G_{VRH}), and Young (E_{VRH}) moduli, the Poisson's ratio (ν) and percentage of anisotropy derived from Voigt-Reuss-Hill approximations [17–19]. From the obtained results, we calculate the Debye temperature (θ_D). Finally, we summarize our outcomes in the last section.

2 Computational method

In this work we have carried out a series of calculations using the CASTEP (Cambridge Serial Total Energy Package) code [20,21], based on density functional theory (DFT) [22,23]. The exchange and correlation function were treated by both the generalized gradient approximation (GGA), as proposed by the Perdew Burke Ernzerhof function (PBE) [24]. First-principles structural and elastic calculations may be performed with sufficient accuracy to resolve energy differences as small as a few meV per atom. Total energy is the primary quantity in first principal calculations [19]. We use the BFGS

[a] e-mail: mromero@ciencias.unam.mx

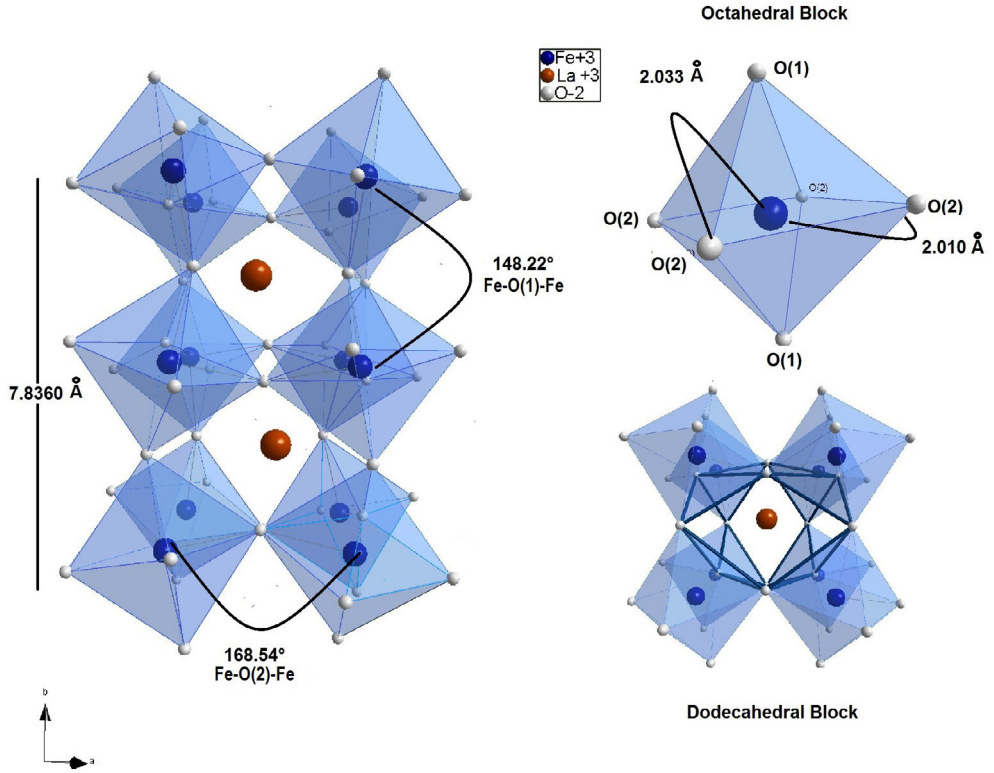

Fig. 1. Crystal structure of the $LaFeO_3$.

(Broyden, Fletcher, Goldfarb, Shanno) algorithm [25] to find the lowest energy of the crystal with an energy tolerance of 2×10^{-6} eV/atom. The first Brillouin zone was sampled on $10 \times 5 \times 10$ irreducible k points [26]. We employ the norm-conserving pseudopotential model [27], with a 990 eV cut of energy. Careful convergence tests show that with these conditions the crystal structure is stable.

3 Results and discussion

3.1 Structural and elastic properties

The members of the $R\mathrm{FeO_3}$ system ($R\mathrm{FeO_3}$ with $R = \mathrm{Y}$, Eu and La) have an orthorhombic symmetry, with space group No. 62 (Pnma), which is a pseudo-cubic space group, and the unit cell parameters are related to the ideal cubic perovskites as $a \sim \sqrt{2}a_p$, $b \sim 2a_p$ and $c \sim \sqrt{2}a_p$, (a_p is the cubic perovskite cell parameter). The Wyckoff positions of atoms are R: $2a$ $(x, 0.25, z)$, Fe: $4b$ (0, 0, 0.5), O(1): $4c$ $(x, 0.25, z)$ and O(2): $8d$ (x, y, z). A good parameter to quantify the stability and distortion of the perovskites structure is the Goldschmidt tolerance factor (t) defined as:

$$t = \frac{r_R + r_\mathrm{O}}{\sqrt{2}(r_\mathrm{Fe} + r_\mathrm{O})}, \tag{1}$$

where r_R is the radius of the R-cation in eight-coordination, r_Fe is the radius of the Fe-cation and r_O is the radius of the oxygen in six-coordination. For the ideal cubic perovskite, this value should be 1.

In the orthoferrites, the distortion mechanism is a tilting of rigid FeO_6 octahedra (see Fig. 1). From the crystallographic point of view, the octahedral tilt angles are directly related to ⟨Fe-O(1)-Fe⟩ and ⟨Fe-O(2)-Fe⟩ bond angles. The former is the tilting angle (θ) of the octahedron relative to the plane [101] and the latter is the rotation angle (ϕ) relative to the plane [010]. The octahedral tilt angles are defined by [28].

$$\theta = \frac{180 - \langle \text{Fe-O(1)} - \text{Fe} \rangle}{2} \tag{2}$$

and

$$\cos\phi = \frac{180 - \langle \text{Fe-O(2)} - \text{Fe} \rangle}{2} / \sqrt{(}\cos\theta). \tag{3}$$

Another quantity used to quantify the distortion of the [FeO_6] octahedron, is the distortion parameter Δ_{oct} defined as:

$$\triangle_{oct} = \frac{(\Sigma\,|(\text{Fe-O}i) - \langle \text{Fe-O} \rangle_\text{average}|)}{\langle \text{Fe-O} \rangle_\text{average}}, \tag{4}$$

where $\langle \text{Fe-O} \rangle_\text{average}$ is an average bond length.

The structure of each phase was optimized with respect to internal parameters, of energy, force, stress, and displacement. The calculated equilibrium cell parameters, unit-cell volume and the Goldschmidt tolerance factor (t) are displayed in Table 1. The atomic positions are shown in Table 2 while the distortion parameter Δ_{oct} and the octahedral tilt angles are listed in the Table 3.

Table 1. Calculated equilibrium cell parameters, unit-cell volume and the Goldschmidt tolerance factor (t). R^{3+} ionic radii ($r_{R^{3+}}$) values given in a ninefold coordination from [29].

Phase	$r_{R^{3+}}$ (Å)	a (Å)	b (Å)	c (Å)	V (Å^3)	t	Ref.
$YFeO_3$	1.075	5.5961	7.6098	5.2855	225.08	0.82	This work
		5.5877	7.5951	5.2743	223.84		[30]
		5.5840	7.5970	5.2740	223.73		[31]
		5.5930	7.6040	5.2820	224.64		[32]
$EuFeO_3$	1.120	5.6060	7.6932	5.3786	231.97	0.91	This work
		5.6060	7.6850	5.3720	234.37		[33]
		5.6810	7.6810	5.3710	231.44		[34]
$LaFeO_3$	1.216	5.5676	7.8364	5.5596	242.59	0.94	This work
		5.5878	7.5775	5.6234	238.10		[35]
		5.5680	7.8360	5.5600	243.31		[36]
		5.5676	7.8608	5.5596	243.32		[37]

Table 2. Atomic positions of the $RFeO_3$ compounds.

Phase	Atom	x	y	z	Ref.
$YFeO_3$	Y	0.0683	0.25	0.9824	This work
		0.06852	0.25	0.98213	[30]
	O(1)	0.4572	0.25	0.1123	This work
		0.4604	0.25	0.1103	[30]
	O(2)	0.6951	−0.0580	0.3082	This work
		0.6955	−0.0567	0.3076	[30]
$EuFeO_3$	Eu	0.0599	0.25	0.9855	This work
		0.0601	0.25	0.9855	[33]
	O(1)	0.0901	0.25	0.4695	This work
		0.4680	0.25	0.0978	[33]
	O(2)	0.2942	0.0463	0.7043	This work
		0.3006	0.0506	0.6977	[33]
$LaFeO_3$	La	0.0291	0.25	−0.0061	This work
		0.0491	0.25	−0.0038	[35]
	O(1)	0.4942	0.25	0.1001	This work
		0.2941	0.25	0.2401	[35]
	O(2)	0.2401	0.0132	0.6983	This work
		0.3406	0.0227	0.6568	[35]

Figure 2 shows the cell parameters as a function of the R^{3+} ionic radii. The b and c cell parameters increased, whereas a cell parameter decreased, as the ionic radius of R^{3+} increased; as a consequence, an increase in the unit-cell volume (V) is observed. Also, from Table 2, the increase of the unit-cell volume induces a Goldschmidt tolerance factor (t) increase. From Table 3, the calculated values of tilt angles θ[101] and ϕ[010] for the $YFeO_3$ are 18.60 and 12.10; respectively, which are in close agreement with the reported values ($\theta_{[101]} = 18.15$ and $\phi_{[010]} = 12.05$) [30].

Several methods are available to compute elastic constants, and in this work we use the finite strain method, which is the most commonly used one. In this approach, the ground state structure is strained according to symmetry-dependent strain patterns with varying amplitudes, followed by a computation of the stress tensor after re-optimization of the internal structure parameters, i.e., after a geometry optimization with fixed cell parameters. The elastic constants are the proportionality coefficients relating the applied strain to the computed stress, $\sigma = C_{ij}\varepsilon_j$. For the orthorhombic crystals there are nine elastic stiffness constants, $C_{11}, C_{22}, C_{33}, C_{44}, C_{55}, C_{66}, C_{12}, C_{13}$ and C_{23} [38].

Table 3. Geometrical parameters characterizing the crystal structure of the $RFeO_3$ compounds.

Bond length (Å)	$YFeO_3$	$EuFeO_3$	$LaFeO_3$
Fe-O(1):2	2.007	1.995	2.036
Fe-O(2):2	2.010	1.997	1.736
Fe-O(2):2	2.033	2.014	2.218
⟨Fe-O⟩	2.017	2.002	1.997
Δ(Fe-O)	6.63×10^{-5}	3.62×10^{-5}	0.020
Bond angle (degrees)			
⟨Fe-O(1)-Fe⟩	142.81	149.13	148.23
⟨Fe-O(2)-Fe⟩	144.32	151.20	168.54
θ[101]	18.60	15.44	15.89
ϕ[010]	12.10	9.41	11.53

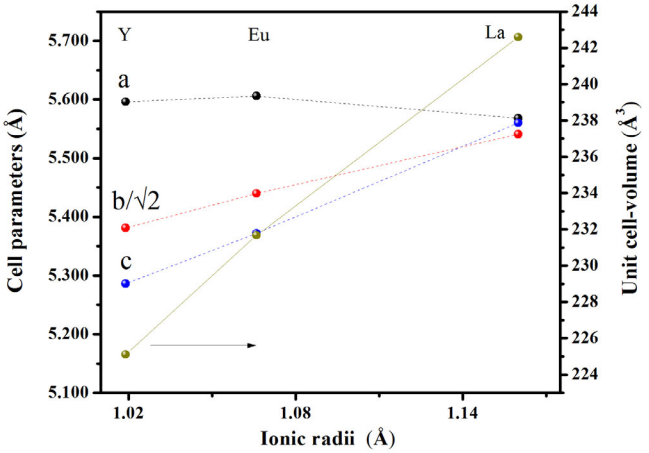

Fig. 2. Cell parameters and Unit cell-volume in a function of R^{3+} ionic radii.

Table 4 shows all the positive elastic constants that satisfy the well-known Born criteria for the mechanical stability: $C_{11}+C_{22} > 2C_{12}, C_{33}+C_{22} > 2C_{23}, C_{11}+C_{33} > 2C_{13}, C_{ii} > 0$ ($i = 1$ to 9) and $C_{11} + C_{22} + C_{33} + 2C_{12} + 2C_{23} + 2C_{13} > 0$. Using the calculated elastic constants we can obtain for monocrystals the macroscopic mechanical parameters: the bulk (B_{VRH}) and shear (G_{VRH})

Table 4. Elastic constants (C_{ij}) of the RFeO$_3$ compounds. The Units GPa.

Phase	C_{11}	C_{22}	C_{33}	C_{44}	C_{55}	C_{66}	C_{12}	C_{13}	C_{23}
YFeO$_3$	243	169	232	113	75	78	113	99	117
EuFeO$_3$	331	346	302	112	116	75	146	160	143
LaFeO$_3$	226	190	254	69	45	66	103	88	115

Table 5. Bulk modulus (B_{VRH}), shear modulus (G_{VRH}), averaged compressibility (β_{VRH}), Young's modulus (E_{VRH}), Poisson's ratio (ν_{VRH}), percentage of anisotropy (A_1), (A_2) and (A_3) of the RFeO$_3$ compounds. The Units in GPa.

Phase	B_{VRH}	G_{VRH}	$\beta_{VRH} \times 10^{-3}$	E_{VRH}	ν_{VRH}	A_1	A_2	A_3
YFeO$_3$	144, 102[a]	56	6.94	148	0.328	1.629	1.802	1.671
EuFeO$_3$	208, 241[b]	94	4.81	246	0.304	1.434	1.277	0.784
LaFeO$_3$	142, 172[c]	59	7.04	155	0.318	0.908	0.848	1.260

[a]Reference [39], [b]reference [40], [c]reference [41].

moduli, which are determined using the Voigt (V) [17] and Reuss (R) [18] approximations.

In the framework of the polycrystalline materials, we utilized the Voigt-Reuss-Hill (VRH) approximation [19]. In this approach, the bulk modulus (B_{VRH}) and the shear modulus (G_{VRH}) are calculated from B_V, B_R, G_V and G_R as: $B_{VRH} = \frac{1}{2}(B_R + B_V)$ and $G_{VRH} = \frac{1}{2}(G_R + G_V)$. The averaged compressibility (β_{VRH}), Young's moduli (E_{VRH}), and Poisson's ratio (ν), can be obtained using these values

$$\beta_{VRH} = \frac{1}{B_{VRH}} \tag{5}$$

$$E_{VRH} = \frac{9B_{VRH}G_{VRH}}{3B_{VRH} + G_{VRH}} \tag{6}$$

and

$$\nu_{VRH} = \frac{3B_{VRH} - 2G_{VRH}}{2(3B_{VRH} + G_{VRH})}. \tag{7}$$

The parameters mentioned above, listed in Table 4 allowed us to make the following predictions. Among RFeO$_3$ phases, EuFeO$_3$ is the phase with the largest bulk modulus (B$_{VRH}$, 208 GPa) and shear modulus (G$_{VRH}$, 94 GPa) while the YFeO$_3$ and LaFeO$_3$ phases have the smallest B$_{VRH}$ ∼144 GPa and G_{VRH} ∼ 56 GPa. As the bulk modulus gives the measure of its stiffness, one may conclude that for the materials of interest, the YFeO$_3$ and LaFeO$_3$ phases show a smaller stiffness compared to the EuFeO$_3$ phase. Furthermore, the average compressibility shows that the Y and La are equally compressible, in the case where Eu is less compressible, which agrees with the values of the elastic constants and the bulk modulus. Figure 3 displays the variation of the G$_{VRH}$/B$_{VRH}$ and Poisson ratio (ν_{VRH}) as a function of ionic radii. According to Pugh criteria, a material should behave in a ductile manner if $G_{VRH}/B_{VRH} < 0.5$, otherwise it should be ductile: according to this indicator, the RFeO$_3$ for R = Y, Eu and La will behave in a ductile manner. The covalent/ionic nature of the compounds could be predicted by the Poisson ratio criterion (ν).

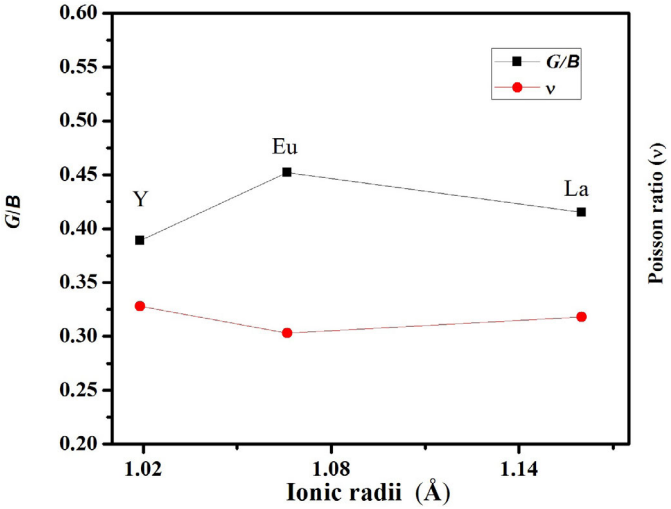

Fig. 3. G/B and Poisson ratio for the RFeO$_3$ compounds.

The representative value of ν is 0.25 for ionic materials while a smaller 0.1 value of is approximated for covalent materials. In the present case, our values are all greater than 0.30 and increase from 0.303 (EuFeO$_3$) to 0.328 (YFeO$_3$) (see Tab. 5). This result represents that the ionic contributions to the atomic bonding are dominant.

Other relevant parameters are the elastic anisotropy factors. The shear anisotropic factors provide a measure of the degree of anisotropy of the bonding between atoms in different planes. An orthorhombic crystal can be measured by three shear anisotropy factors for the {100}, {010} and {001} shear planes, respectively [42]:

$$A_1 = \frac{4C_{44}}{C_{11} + C_{33} - 2C_{13}}, \tag{8}$$

$$A_2 = \frac{4C_{55}}{C_{22} + C_{33} - 2C_{23}}, \tag{9}$$

and

$$A_3 = \frac{4C_{66}}{C_{11} + C_{22} - 2C_{12}}. \tag{10}$$

Table 6. Debye temperature (θ_D) and velocity of sound (v_m) of RFeO$_3$ compounds.

Phase	v_m (m/s)	θ_D (K)	Ref.
YFeO$_3$	3381	449	This Work
EuFeO$_3$	4643	505	”
LaFeO$_3$	3911	415, 407 [a]	”

[(a)] Reference [46].

For an isotropic crystal, the A_1, A_2 and A_3 factors should be equal; any lower or higher value than unity is a measure of the degree of anisotropic elasticity possessed by the crystal. Table 5 shows the calculated values of A_1, A_2 and A_3. It is interesting to note that the shear anisotropic factors show a higher degree of anisotropy for YFeO$_3$, EuFeO$_3$ and LaFeO$_3$ respectively, implying a lower charge density between the junctions of different planes in all three compounds.

Another elastic quantity is the hardness, which quantifies the resistance to deformation, this is defined as [43]:

$$H_v = 0.92K^{1.137}G^{0.708}, K = G_{VRH}/B_{VRH}, \quad (11)$$

The obtained hardness (Vickers number) is 5.43, 9.30 and 6.07 for R = Y, Eu and La, respectively.

Among the important fundamental parameters, which are closely related to many of the physical properties of solids is the Debye temperature (θ_D). Using the elastic moduli G$_{VRH}$ and B$_{VRH}$, we calculated the Debye temperature (θ_D) [44] as:

$$\theta_D = \left[\frac{h^3}{k^3}\frac{3N}{4\pi V}\right]^{1/3} v_m, \quad (12)$$

where V is the unit cell volume, N is the number of atoms in the unit cell, k is Boltzmann's constant and h is Plank's constant. The average sound velocity v_m is given by reference [45]:

$$v_m = \frac{3^{1/3}(3G_{VRH}B_{VRH} + 4{G_{VRH}}^2)^{1/2}}{\rho^{3/2}(2(2B_{VRH} + 4G_{VRH})^{3/2} + 3G_{VRH}^{3/2}}. \quad (13)$$

Table 6 shows the Debye temperature calculated from the elastic constants for the RFeO$_3$ system. Debye temperature data for EuFeO$_3$ and YFeO$_3$ are not available in the literature, only for LaFeO$_3$ [46].

4 Conclusions

In summary, we performed calculations of structure and elasticity of the RFeO$_3$ with R = Y, Eu, and La phases, using a plane-wave pseudopotential density functional theory, within the generalized gradient approximation. We find that the reduction of ionic radii produces a decrease of the unit cell-volume; as a consequence the bond lengths associated with the [FeO$_6$] octahedra and the octahedral distortion decrease. Our analysis of elastic constants (C_{ij}) shows that our system is mechanically stable. Analyzing the ratio of bulk moduli and shear modulus we conclude that the RFeO$_3$ system is ductile in nature. Finally, no correlation between the ionic radius and the Debye temperature is observed.

Partial support for this work was provided by the project IN 115612, and the Programa de Becas Posdoctorales de la UNAM, DGAPA, UNAM. The authors want to thank C. Gonzalez for their technical support. Calculations were done using resources from the Supercomputing Center DGTIC-UNAM.

References

1. Mineral Data Publishing, version 1, (2005)
2. N.N. Toan, S. Saukko, V. Lantto, Physica B **327**, 279 (2003)
3. N.Q. Minh, J. Am. Ceram. Soc. **76**, 563 (1993)
4. I. W rnhus, P.E. Vullum, R. Holmestad, T. Grande, K. Wiik, Solid State Ionics **176**, 783 (2005)
5. F. Bidrawn, S. Lee, J.M. Vohs, R.J. Gorte, J. Electrochem. Soc. **155**, B660 (2008)
6. N.A. Spaldin, Topics Appl. Phys. **105**, 175 (2007)
7. D.I. Khomskii, J. Magn. Magn. Mater. **306**, 1 (2006)
8. J.F. Scott, Nat. Mater. **6**, 256 (2007)
9. J.F. Craig, K.M. Rabe, Phys. Rev. Lett. **97**, (2006)
10. June Hyuk Lee et al., Nat. Lett. **466**, 954 (2010)
11. A. Wu, H. Shen, J. Xu, Z Wang, L. Jiang, L. Luo, S. Yuan, S. Cao, H. Zhang, Bull. Mater. Sci. **35**, 259 (2012)
12. A.V. Soldatov, N.A. Povahzynaja, I.G. Shvejtzer, Solid State Commun. **97**, 53 (1996)
13. J. Luning, F. Nolting, A. Scholl, H. Ohldag, J.W. Seo, J. Fompeyrine, J.-P. Locquet, J. Stohr, Phys. Rev. B **67**, 214433 (2003)
14. S. Qing-Gong, L. Li-Wei, Z. Hui, Y. Hui-Yu, D. Quan-Guo, Acta Physica Sinica **61**, 107102 (2012)
15. Q. Zhang, S. Yunoki, J. Phys.: Conf. Ser. **400**, 032126 (2012)
16. N. Singh, J.Y. Rhee, J. Korean Phys. Soc. **53**, 806 (2008)
17. W. Voigt, *Lehrbuch der Kristallphysik* (Teubner, Leipzig, 1928), pp. 739−754
18. A. Reuss, Z. Angew, Math. Mech. **9**, 49 (1929)
19. R. Hill, Proc. Phys. Soc. **65**, 349 (1952)
20. S.J. Clark, M.D. Segall, C.J. Pickard, P.J. Hasnip, M.J. Probert, K. Refson, M.C. Payne, Z. Kristallogr. **220**, 567 (2005)
21. M.D. Segall, P.J.D. Lindan, M.J. Probert, C.J. Pickard, P.J. Hasnip, S.J. Clark, M.C. Payne, J. Phys.: Condens. Matter **14**, 2717 (2002)
22. W. Kohn, L.J. Sham, Phys. Rev. A **140**, 1133 (1965)
23. M.C. Payne, M.P. Teter, D.C. Allan, D.C. Allan, T.A. Arias, J.D.J. Joannopoulos, Rev. Mod. Phys. **64**, 1045 (1992)
24. J.P. Perdew, K. Burke, M. Ernzerhof, Phys. Rev. Lett. **77**, 3865 (1996)
25. B. Pfrommer, G.M. Cote, S.G. Louie, M.L. Cohen, J. Comput. Phys. **131**, 233 (1997)
26. H.J. Monkhorst, J.D. Pack, Phys. Rev. B **13**, 5188 (1976)
27. D.R. Hammann, M. Schluter, C. Chiang, Phys. Rev. Lett. **43**, 1494 (1979)

28. Y.S. Zhao, D.J. Weidner, J.B. Parise, D.E. Cox, Phys. Earth Planet. Inter. **17**, 17 (1993)
29. R.D. Shannon, Acta Crystallogr. A **224**, 751 (1976)
30. D. du Boulay, E.N. Maslen, V.A. Streltsov, N. Ishizawa, Acta Crystallogr. B **51**, 921 (1995)
31. R. Maiti, S. Basu, D. Chakravorty. J. Magn. Magn. Mater. **321**, 3274 (2009)
32. K.T. Jacob, G. Rajitha, Solid State Ionics **32**, 32 (2012)
33. M. Marezio, J.P. Remeika, P.D. Dernier, Acta Crystallogr. B **26**, 2008 (1970)
34. G.J. McCarthy, R.D. Fischer, J. Solid State Chem. **4**, 340 (1972)
35. M. Marezio, P.D. Dernier, Mater. Res. Bull. **6**, 23 (1971)
36. L. Mark, *Crystal structure and defect property predictions in ceramic material* (Imperial College, London, 2005)
37. M. Romero, R.W. Gómez, V. Marquina, J.L. Pérez-Mazariego, R. Escamilla, Physica B **443**, 90 (2014)
38. J.F. Nye, *Physical Properties of Crystals* (Claredon Press, Oxford, 1985)
39. M. Derras, N. Hamdad, Results Phys., **3**, 61 (2013)
40. G. Kh. Rozenberg, M.P. Pasternak, W.M. Xu, L.S. Dubrovinsky, S. Carlson, R.D. Taylor, Europhys. Lett. **71**, 228 (2005)
41. M. Etter, M. Muller, M. Hanfland, R.E. Dinnebier, Acta Crystallogr. B **70**, 452 (2014)
42. D.H. Chung, W.R. Buessem, F.W. Vahldiek, in *Anisotropy in Single Crystal Refractory Compounds*, edited by S.A. Mersol (Plenum Press, New York, 1968), p. 217
43. Y. Tian, B. Xu, Z. Zhao, Int. J. Refract. Metals and Hard Mater. **33**, 93 (2012)
44. L.O. Anderson, Phys. Chem. Solids **24**, 909 (1963)
45. J.P. Poirier, *Introduction to the Physics of the Earth's Interior* (Cambridge University Press, 2000)
46. S.C. Parida, S. K Rakshit, Ziley Singh, J. Solid State Chem. **181**, 101 (2008)